



A density functional theory study of the mechanisms and energetics of graphene-like structures growth on palladium

Matías A.O.Quiroga^{1*}, Gabriela F.Cabeza¹, Miguel D.Sánchez^{1,2}

¹Grupo de Materiales y Sistemas Catalíticos, Departamento de Física, Universidad Nacional del Sur, Avda. Alem 1253, B8000CPB Bahía Blanca, (ARGENTINA)

²Planta Piloto de Ingeniería Química, La Carrindanga km 7, 8000 Bahía Blanca, (ARGENTINA)

E-mail: mquiroga@uns.edu.ar

Received: 31st May, 2011 ; Accepted: 30th June, 2011

ABSTRACT

Density functional theory studies were performed to understand the early stage of graphene like structures nucleation and growth on Pd. The adsorption of C atoms on four Pd(111) surface models was examined. We found adsorption energies ranging from -479 kJmol^{-1} , for a top site on a Pd(111) surface, to -804 kJmol^{-1} , for a hollow-hcp site for Pd_{step-edge}(111) surfaces. Local density of state curves analysis showed significant carbon/palladium bond hybridization. When incorporating new C atoms, these were attracted by the adatoms simulating a hexagonal ring. The calculations using a surface model containing steps, terrace and clusters suggested that the nucleation of atomic C is promoted.

© 2011 Trade Science Inc. - INDIA

KEYWORDS

Density functional calculations;
Carbon chemisorption;
Palladium catalyst;
C rings;
Graphene.

INTRODUCTION

The general nucleation and growth mechanism of carbon nanomaterial, in a CVD (Chemical Vapor Deposition) process assumes the hydrocarbon molecule dissociation (catalyzed by the transition metal) and dissolution, as well as saturation of carbon atoms in the metal nanoparticle. Within this scheme we can see two different growth patterns, the “tip-growth” and the “base-growth”^[1]. The metal–support interactions are found to play a defining role for the growth mechanism^[2]. Weak interactions yield tip-growth mode whereas strong interactions lead to base-growth mode.

The tip-growth model involves the carbon diffusion through the metallic nanoparticle and the subsequent

detachment of the particle from the substrate, being the driving force of this process attributed to either the temperature gradient or the carbon concentration gradient between the gas-metal and particle-substrate interfaces^[3-5]. On the other hand, the base-growth model implies the formation of a graphitic layer on the curved metal surface with the addition of carbon atoms or dimers from the particle base^[6,7].

By means of time resolved HRTEM (high resolution in situ transmission electron microscope) observations, Helverg *et al.* visualized the dynamics of solid-gas interaction at atomic level in the CNF formation by methane decomposition over supported nickel catalyst^[8]. Their results, supported by density functional theory (DFT) calculations, are consistent with a growth model

Full Paper

involving surface transport of carbon and nickel atoms. The nucleation and growth of carbon structures layers are associated with the dynamic formation and restructuring of monatomic step-edges on the nickel surface. The authors indicate that, while in some growth conditions the carbon diffusion could proceed through the Ni particle, it is not necessary to consider a bulk diffusion model to achieve a coherent image. The specific role of the nanocluster surface has also been considered by other authors who proposed different growth models based on surface carbon transport^[9-13].

Recent studies of Esconjauregui *et al.*^[14] on the reasons why metals catalyze the nucleation and growth of carbon nanomorphologies propose that metals with few d-vacancies such as Ni, Co, or Fe are the best catalysts to nucleate and grow carbon nanotubes (CNTs) as they can both form metastable carbides and release carbon atoms under typical CNT synthesis conditions. Metals with a large number of d-vacancies are active catalysts only if their stable carbides can decompose carbon sources whereas metals with full d-orbitals are active catalysts only at the nanoscale (nanoparticles 1 nm or smaller).

In a previous paper we investigated the carbon nanofiber formation over alumina supported Pd catalyst in the reforming reaction of methane with carbon dioxide^[15]. Our characterization by HRTEM showed the formation of nanofibers with diameters ranging between 8 and 18 nm and different orientation of the graphitic layers (but mainly hollow fishbone type). We have determined that the growth of the fiber is related to the formation of a few graphitic layers that surround the metal particle.

With the aim of GGA-DFT calculus, L. Gracia *et al.*^[16] studied the diffusion of C in palladium surface and subsurface, finding that the insertion of C is energetically favourable, being the subsurface C preferentially trapped in octahedral sites with a gain in energy of 690 kJmol⁻¹ and the horizontal migration takes place between octahedral and tetrahedral sites below the first Pd surface layer and the most favourable path involves a barrier of 71 kJmol⁻¹. Diffusion to the bulk was found to be an energetically costly process.

Meanwhile, in a recent work L. Nykänen *et al.*^[17] by means of RPBE-DFT calculus, have found that the C adsorption in the bulk is more stable than on the Pd surface. On the other hand, Hu *et al.*^[18] performed DFT

studies of transition metal adatoms adsorbed on graphene and mentioned the special case of Pd that is different from other transition metals. While the Pd atom adsorption on graphene is a chemisorption, graphene adsorption on Pd substrate is a physisorption. However, P. A. Khomyakov *et al.*^[19] by using LDA-DFT and analyzing band structures, found that graphene is chemisorbed on the Ni, Co or Pd (111), or on the Ti (0001) surface.

The main discussion can be summarized as follows: (i) there may exist differences between the chemical behaviour of a single C atom and graphene-like structures over Pd surface; (ii) the obtained results mostly depends upon the choice of the exchange-correlation functional.

In this work, we present density functional theory (DFT) calculations to understand the origin of the interface process that takes place during the early stage of the nucleation and growth of graphene-like structures on Pd surfaces. The paper is organized as follows: section 2 describes the theoretical framework and section 3 the slab models used. In section 4, divided into two subsections, we present our results and discussion. Finally, our conclusions are given in section 5.

COMPUTATIONAL DETAILS

Density Functional calculations were performed with the *Vienna Ab Initio Simulation Package* (VASP)^[20-22]. The Kohn-Sham one-electron wave functions were expanded on a basis of plane waves with cutoff value of 500 eV for the kinetic energy. The exchange-correlation functional was treated according to the Generalized Gradient Approximation (GGA) in the parameterization of Perdew–Wang (PW91)^[23]. Previous studies^[24] and present tests do not reveal any noticeable spin polarization effect for neither the substrate Pd models nor the adsorption atoms on them. Thus, all calculations (except for the free carbon atom) were spin-restricted.

The interaction between atomic cores and valence electrons was described by the projector augmented wave (PAW) method^[25,26]. For the PAWs we considered ten valence electrons for Pd (3d⁹4s¹) and four for C (2s²2p²). The blocked Davidson approach was applied as the electronic minimization algorithm. We used Monkhorst-Pack kpoint mesh^[27] and the Methfessel-

Paxton technique^[28] with a smearing factor of 0.2 for the electronic levels. The convergency of the k-point mesh was checked by increasing the k-point mesh until the energy has converged with a precision better than 1 meV/atom. In this way the size of the kpoint mesh considered was 5x5x1.

Structures were optimised until the maximum forces acting on each atom became less than 10 meV/Å. The electronic structure for C adsorbed was analyzed in terms of Density of States (DOS).

SLAB MODELS

An FCC stacking layered structure was assumed for the calculations. The reference Pd(111) surface was represented by four-layer slabs. Preliminary tests with slab models containing up to five atomic layers have shown that a slab with four layers provides converged results; the difference in the surface energy between four and five layer-slabs was about 0.005 eV. The repeated atom slabs were separated in z direction by a vacuum region equivalent to five interlayer spaces optimized to avoid the interaction between them. Atom positions in the bottom three layers were kept frozen as optimized for Pd bulk, whereas the other layer (closer to adsorbate) was allowed to relax completely, within a maximum force criterion of 0.01 eV/Å providing an interatomic distance relaxation of 1.4 %. The cell parameter was calculated to be 2.79 Å. As it could be expected, calculated GGA bond distances are longer than the respective experimental value (2.75 Å).

With the aim of standing for the surface roughness, four different Pd model surfaces were investigated. A plane surface, modeled by the close-packed Pd(111) surface with a p(2x2) unit cell (Figure 1a); a stepped surface with two atomic rows missing (Pd_{step-edge}) represented with a (3x2) unit cell (Figure 1b); a terrace surface (Pd_{terrace}) modeled with a (4x2) unit cell (Figure 1c); and a four Pd atoms cluster surface (Pd_{cluster}) on a Pd(111) surface modeled with a (5x5) unit cell (Figure 1d). Both stepped model surfaces (Figure 1b and 1c) have a slab thickness comparable to the Pd(111) surfaces.

RESULTS AND DISCUSSION

The current section was divided into two parts. Section 4.1, presents the calculated adsorption ener-

gies at different sites for low coverages ($\theta \leq 0.25$ ML) and two transport paths for carbon are examined. In section 4.2, we describe the growth of graphene like structures and finally we analyze the carbon adsorption energies at high coverages ($\theta > 0.25$ ML).

C monoatomic adsorption and diffusion on Pd(111) surfaces

Here, we examined the carbon stability at different sites. The C monoatomic adsorption on Pd(111) corresponding to a coverage of 0.25 ML (one C per four Pd atoms exposed on the surface) was calculated at four possible sites: top (T), bridge (B) and two hollow sites, tetrahedral (H_{tet}) and octahedral (H_{oct}) as indicated in Figure 1a. To study the C adsorption on Pd_{step-edge}(111) surface corresponding to coverage of 0.17 ML (one C per six Pd atoms exposed on the surface) we added three more sites: one adatom above a single Pd atom of the monoatomic step-edge, denoted as T_{SE}, a bridge site between two Pd atoms of the monoatomic step-edge (B_{SE}) and a third one corresponding to a C adsorbed on the corner between the terrace and the step-edge (B_C) (Figure 1b). Similar sites considered for the study of C adsorbed on Pd_{terrace} and Pd_{cluster} are schematized in Figures 1c and 1d.

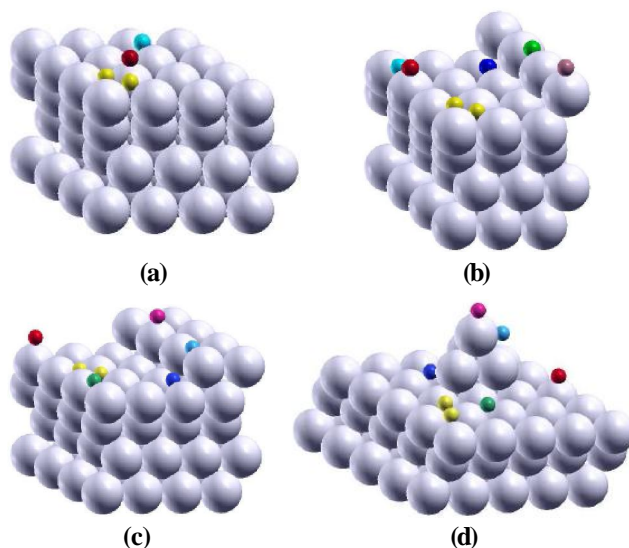


Figure 1 : Four different Pd model surfaces used in the calculations. (a) plane Pd(111) surface; (b) Pd_{step-edge} (stepped surface with two atomic rows missing); (c) Pd_{terrace}; (d) Pd_{cluster} (cluster of four Pd atoms deposited on the Pd(111) surface). The sites correspond to: T (red), B (turquoise), H_{tet} and H_{oct} (yellow); for Pd_{step-edge} surface we include the sites: T_{SE} (violet), B_{SE} (green) and B_C (blue).

The C adsorption energy by atom (E_{ads}) was cal-

Full Paper

culated as follows:

$$E_{\text{ads}} = (E_{\text{C}_n\text{Pd}} - E_{\text{Pd}} - nE_{\text{C}})/n \quad (1)$$

where $E_{\text{C}_n\text{Pd}}$ is the total energy of the adsorption system; E_{Pd} is the total energy of the clean Pd(111) surface; E_{C} is the total energy of an isolated C atom and n is the number of C atoms adsorbed; in this section we discuss the situation for $n = 1$. The adsorption energies and geometry information are summarized in TABLE 1. We found that the hollow sites were more energetically favorable than the bridge and top ones in both analyzed cases in good agreement with that reported in reference^[29]. As mentioned in Section 2, the physical consequences of the magnetic nature of this effect for C adsorption was not noticeable as suggested by a margin of 0.5 % between the adsorption energy values obtained for non-spin polarized (NSP) and spin polarized (SP) calculations. Comparing both surfaces, the adsorption of C on the step was slightly favored by 8 % in contrast to the flat surface.

In order to improve the knowledge of the models used, the respective *formation energy* for Pd_{step-edge}, Pd_{terrace} and Pd_{cluster} were calculated. The obtained values were: -197 kJmol⁻¹, -465 kJmol⁻¹ and -436 kJmol⁻¹, respectively. Starting from these formation energies we can explain, for example, the observed spontaneous palladium step-edges formation: the step-edge formation energy is less than the energy gained when carbon atoms bind to the step-edges. These results were concordant with those reported by other authors using different models and approximations^[30-32].

TABLE 1 : Binding energies (kJmol⁻¹) and interatomic distances (Å) of C adsorption on Pd(111) surfaces. The sites correspond to: top (T), bridge (B) and two hollow sites (H_{tet} and H_{oct}); for Pd_{step-edge}, Pd_{terrace} and Pd_{cluster} surfaces we included the sites: T_{SE}, B_{SE} and B_C (see text and Figure 1).

Site	Pd θ = 0.25 ML		Pd _{step-edge} θ = 0.17 ML		Pd _{terrace} θ = 0.125 ML		Pd _{cluster} θ = 0.04 ML	
	Z _{C-Pd}	E _{ads}	Z _{C-Pd}	E _{ads}	Z _{C-Pd}	E _{ads}	Z _{C-Pd}	E _{ads}
T	1.80	-479	1.80	-594	1.80	-603	1.80	-481
T _{SE}	-	-	1.80	-512	1.71	-568	1.71	-546
B	1.84	-671	1.84	-683	1.84	-669	1.84	-673
B _C	-	-	1.84	-112	1.83	-132	1.84	-211
B _{SE}	-	-	1.44	-693	1.68	-690	1.82	-609
H _{oct}	1.90	-732	1.90	-786	1.90	-770	1.90	-732
H _{tet}	1.90	-740	1.90	-804	1.90	-791	1.90	-738

The monoatomic C adsorption on Pd can be analyzed in terms of the *electronic structure* evaluating

the local density of states (LDOS) obtained by projection of the wave functions on an atomic basis. We will do this for the hollow configuration as it is the most stable. For that purpose the partial LDOS (3d band) for the surface Pd atom closer to C adsorbed and the LDOS (s+p bands) of the C adatom are exhibited in Figure 2. We can observe the contrast between clean Pd d-band and free C (s+p) bands with the corresponding one after interaction. The C adsorption induces a loss of states in the region (0.5; -2.5 eV), a gain of states in the region (-2.5; -5 eV) and new states in the range (-6; -5 eV), as well as one centered around -11 eV (Figure 2a). Whereas for a free C atom (Figure 2b), there are two peaks centered around -8 and 0 eV. After the adsorption, the first one was shifted -3 eV and the second one is characterized by a large splitting of (s + p) states with two main structures around -5 and 1 eV. This could represent bonding and anti-bonding states, respectively. Therefore, the LDOS analysis accounts for a strong hybridization of adsorbate (s + p) states with the local states of surface Pd atoms. These are indications of strong covalent C–Pd bonding. Likewise, the splitting caused by hybridization reduces the LDOS around the Fermi level for Pd atoms, which have direct covalent bonds with the adsorbate. Theoretical calculations for C and S on Pd(533) and Pd(320)^[33] also showed a large splitting of p states of C and S with two main structures separated by 7-8 eV. The differences between the electronic environment of step-edge Pd atoms obtained from the density of state curves were not noteworthy, and therefore not presented here.

The *center of gravity of the d-states*, e_d , defined as the DOS centroid in an atomic sphere centered at a surface atom, was evaluated in order to characterize the surface d-electron ability of taking part in the bonding with the adsorbate. We observed that the C-substrate interaction shifts the pure Pd d-band centroid towards higher binding energies by approximately 1 eV. Additionally, when the Pd d-band is placed near atomic orbitals the chemisorption strength increases, verifying the correlation between d-band position and chemisorption strength^[34].

As described above, the hollow sites are more energetically favorable than the bridge and top ones. Therefore, the C adsorption at H_{oct} site and H_{tet} site is chosen as the initial and final state, respectively, to in-

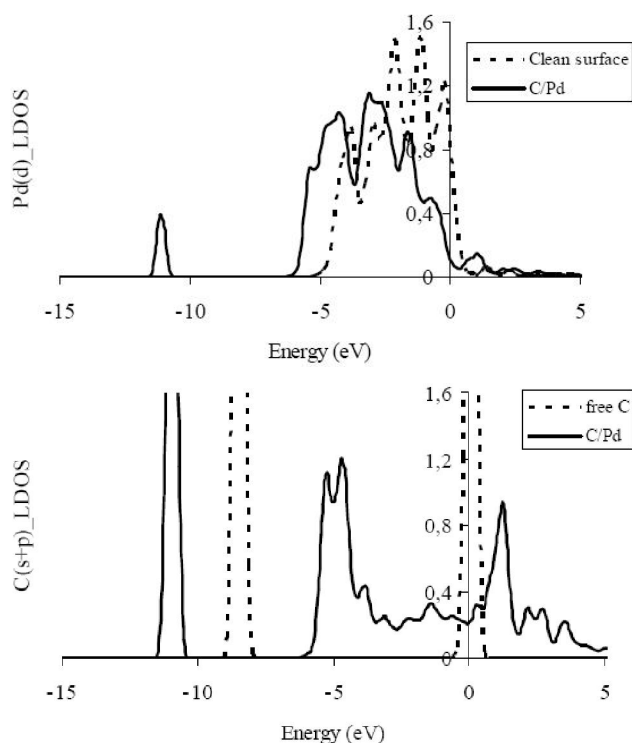


Figure 2 : LDOS corresponding to C-Pd system. (a) Comparison of the Pd d-band before (dashed line) and after (solid line) adsorption of C on hollow site. (b) (s+p) bands for C in the free state (dashed line) and after adsorption (solid line). The Fermi level lies at 0 eV.

investigate the C horizontal diffusion on the surface. The converged minimum energy paths (MEPs) for C diffusion were evaluated along two different paths for both Pd(111) and Pd_{step-edge}(111) surfaces. In the first Path, a C atom moves from the H_{oct} to the most stable H_{tet} via a top site; while in second Path it moves along an adjacent bridge sites.

We found that the activation energy for the C diffusion along the first Path were 259 and 211 kJmol⁻¹ for Pd(111) and Pd_{step-edge}(111), respectively. Nevertheless, the calculated energy barriers for the second Path were 69 kJmol⁻¹ and 122 kJmol⁻¹, lower than those along the first Path. This shows that the C adatom preferentially diffuses between hollow sites via bridge site. The respective curves are presented in the Supplementary Information (Figure S1).

Nucleation and growth of graphene-like structures

Up to this point, we have presented the case of monatomic C adsorption on Pd surfaces. What happens when more than one C reaches the surface? We proposed a tentative carbon ring formation adsorbed on Pd(111). With this goal in mind, we used a surface

unit cell (v3xv3) by taking the geometry-optimized configuration of Pd(111) surface. First we placed a C atom on a hollow site (denoted as 1 in Figure 3). Then, a second C (2) was approached keeping an interatomic equilibrium distance of 1.39 Å. The representative unit cell of a graphene layer was obtained by adding consecutively C adatoms denoted as 3, 4, ..., 8. For this ideal situation, the incorporation energy involved in the formation of a C ring was estimated by DFT calculations using the formula:

$$E_{inc_Cn} = E_{Cn_Pd} - E_{Cn-1_Pd} - E_C \quad (2)$$

where E_{Cn_Pd} is the total energy of Pd surface with n C atoms adsorbed (with n = 1 to 8); E_{Cn-1_Pd} is the total energy of Pd surface with (n-1) C atoms adsorbed and E_C is the total energy of an isolated C atom in a box. The corresponding energy profile is also shown in Figure 3.

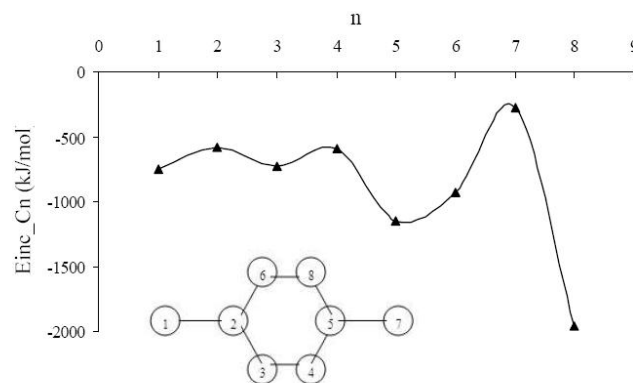


Figure 3 : Energy profile obtained for the corresponding carbon ring formation adsorbed on Pd(111) vs. the number of C atoms incorporated into the ring (n). The bottom of the figure shows a configuration scheme followed by the incorporation of C.

A negative energy value means that the C adatoms were bound to the Pd surface. In spite of the C-C repulsions, the formation of the ring was favored. The procedure included the optimization of the C coordinates in addition to the relaxation of the two surface layers of the slab. The E_{inc} becomes more important as the C ring is being completed. We note that the instability, observed by the addition of the seventh C to the ring, disappears upon completion of the bonds. In turn, the rings might bind together creating a graphited layer. There is a driving force for graphene formation due to the energy gain per incorporated C atom. Independently of the initial nucleation mechanism, the barrier for the incorporation of the first C is small (around 150 kJ/mol) because no covalent bonds are being broken.

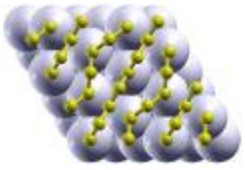
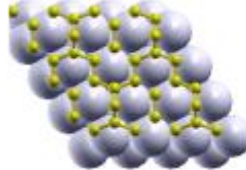
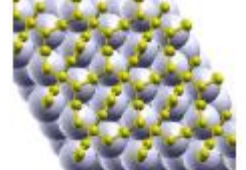
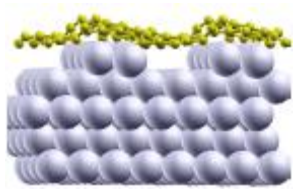
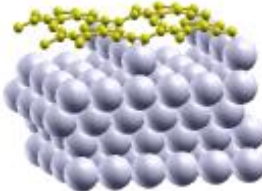
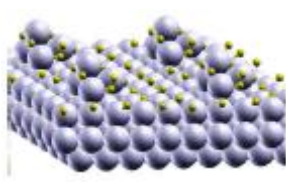
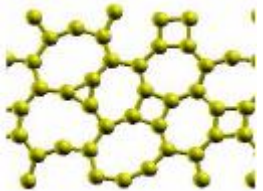
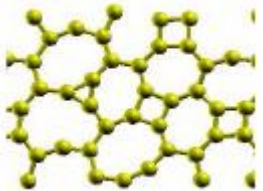
Full Paper

In order to improve the knowledge of the growth of graphene-like structures, we calculated the adsorption energies at *highest coverages* for the models described in section 3. TABLE 2 summarizes the most representative cases and shows sketches of the final states after relaxation. The respective C coverage (expressed in ML) and adsorption energies are shown in *italics and bold*, respectively. The energy values in this table were obtained by using equation (1) with n between 8 and 19 giving rise to the different coverages (see Table S1 in Supplementary Information). The results indicate that the energy increases slightly as the coverage grows. From a coverage of 4 ML, the adsorption energy starts de-

creasing due to a substantial repulsive interaction between the C atoms. The step-edge site preference still persists when compared with the smooth Pd surface for the same coverage. Note the formation of C rings for coverages greater than 2 ML. When the roughness is present on the surface, the C rings layer is curved to fit the steps or the terraces. At higher coverages, the C atoms are stabilized in the terrace hollow sites.

To further understand the effects of substrate in the formation of C rings, we have also relaxed 19 C atoms in a cell without the presence of metal. After relaxation different rings were formed with 4, 6 and 7 carbons (see TABLE 2 last cell).

TABLE 2 : Calculated adsorption energies (in bold) at different coverages (in italics) for the models described in section 3 after relaxation. The respective units are $\text{kJmol}^{-1}/\text{at}$ and ML. The first row corresponds to C adsorption on the smooth Pd surface. The fifth, sixth and seventh cells, correspond to $\text{Pd}_{\text{step_edge}}$, $\text{Pd}_{\text{terrace}}$ and $\text{Pd}_{\text{cluster}}$. In the last cell we present the formation of C rings without metal substrate. Color online: C are shown in yellow and Pd in gray.

2	-758	2.25	-766	4	-763	5.33	-808
							
2.37	-797	2	-802	0.68	-637	----	-807
							
							

CONCLUSIONS

In this work we used DFT calculations to investigate the C chemisorption and diffusion on Pd surface with the aim of understanding the early growth stage mechanism of graphene like structures on Pd based catalysis. For this purpose, five different surface models were studied.

We found that C atoms would bind strongly to the surface, preferably to the threefold hcp sites, with adsorption energies of -740 kJmol^{-1} for Pd(111) and -804 kJmol^{-1} for $\text{Pd}_{\text{step_edge}}$ corresponding to 0.25 and 0.17 ML respectively.

The LDOS calculations showed that C-substrate interaction causes a strong hybridization of adsorbate

(s+p) states with the local states of surface Pd atoms. This was evidenced by the shift of the Pd pure d-band centroid ($\sim 1 \text{ eV}$), and a Pd atoms LDOS reduction around the Fermi level, which have direct covalent bonds with the adsorbate.

The minimum energy path evaluation indicates that the bridge site acts as a transition site for C diffusion between hollow sites with activation barriers of 69 and 122 kJmol^{-1} for 0.25 and 0.17 ML, respectively.

In order to explore the formation of carbon rings, we calculated the adsorption energies at highest coverages. The results show that the energy increases slightly as the coverage grows. From a coverage of 4 ML the adsorption energy starts decreasing due to a substantial repulsive interaction between the C atoms. The step-edge site preference still persists. The formation of car-

bon rings is observed for coverages greater than 2 ML. When the roughness is present at the surface, the rings curve to fit to the steps or the terraces. The C ring formation without substrate also was reported.

The calculations show that the surface irregularities promote the nucleation of C atoms. Pd step-edges can be induced by adsorbed C atoms because the C binding energy to the Pd step-edge is larger than the energy gain of forming a monoatomic step-edge (197 kJmol⁻¹/at). The results suggest that the nucleation and growth of graphene like structures are associated with the dynamic formation and restructuring of monoatomic step-edges at the palladium surface.

ACKNOWLEDGMENTS

This work is supported by the Departamento de Física of UNS, ANPCyT and CONICET. We are grateful to Ing. Fernando A. Caba (Director General de Telecomunicaciones, UNS) for his technical support; to Mg. Verónica Owen and Mg. Andrew Owen for English review. Discussions with Norberto J. Castellani and Ricardo Ferullo are gratefully acknowledged.

REFERENCES

- [1] A.V.Melechko, V.I.Merkulov, T.E.McKnight, M.A.Guillorn, K.L.Klein, D.H.Lowndes, M.L.Simpson; *J.App.Phys.*, **97**, 041301 (2005).
- [2] A.C.Dupuis; *Prog.in Mat.Sci.*, **50**, 929 (2005).
- [3] J.-W.Snoeck, G.F.Froment, M.Fowles; *Growth J.Catal.*, **169**, 240 (1997).
- [4] R.T.K.Baker, M.A.Barber, P.S.Harris, F.S.Feates, R.J.Waite; *J.Catal.*, **26**, 51 (1972).
- [5] M.Pérez-Cabero, E.Romeo, C.Royo, A.Monzón, A.Guerrero-Ruiz, I.Rodríguez, Ramos; *J.Catal.*, **224**, 197 (2004).
- [6] J.-Y.Raty, F.Gygi, G.Galli; *Phys.Rev.Lett.*, **95**, 096103 (2005).
- [7] Y.Li, W.Kim, Y.Zhang, M.Rolandi, D.Wang, H.Dai; *J.Phys.Chem.B*, **105**, 11424 (2001).
- [8] S.Helveg, C.López-Cartes, J.Sehested, P.L.Hansen, B.S.Clausen, J.R.Rostrup, Nielsen, F.Abild-Pedersen, J.K.Nørskov; *Nature*, **427**, 426 (2004).
- [9] T.Baird, J.R.Fryer, B.Grant; *Carbon*, **12**, 591 (1974).
- [10] H.E.Grenga, K.R.Lawless; *J.Appl.Phys.*, **43**, 1508 (1972).
- [11] S.Hofmann, C.Ducati, J.Robertson, B.Kleinsorge; *Appl.Phys.Lett.*, **83**, 135 (2003).
- [12] A.Oberlin, M.Endo, T.Koyama; *J.Cryst.Growth.*, **32**, 335 (1976).
- [13] D.Chen, K.O.Christensen, E.Ochoa-Fernández, Z.Yu, B.Tøtdal, N.Latorre, A.Monzón, A.Holmen; *J.Catal.*, **229**, 82 (2005).
- [14] S.Esconjauregui, C.M.Whelan, K.Maex; *Carbon*, **47**, 659 (2009).
- [15] M.D.Sánchez, M.S.Moreno, I.Costilla, C.E.Gigola; *Cat.Today*, **133-135**, 842 (2008).
- [16] L.Gracia, M.Calatayud, J.Andrés, C.Minot, M.Salmeron; *Phys.Rev.B*, **71**, 033407 (2005).
- [17] L.Nykänen, J.Andersin, K.Honkala; *Phys.Rev.B*, **81**, 075417 (2010).
- [18] Leibo Hu, Xianru Hu, Xuebin Wu, Chenlei Du, Yunchuan Dai, Jianbo Deng; *Physica B*, **405**, 3337 (2010).
- [19] P.A.Khomyakov, G.Giovannetti, P.C.Rusu, G.Brocks, J.van den Brink, P.J.Kelly; *Phys.Rev.B*, **79**, 195425 (2009).
- [20] G.Kresse, J.Hafner; *Phys.Rev.B*, **47**, 558 (1993).
- [21] G.Kresse, J.Hafner; *Phys.Rev.B*, **48**, 13115 (1993).
- [22] G.Kresse, J.Hafner; *Phys.Rev.B*, **49**, 14251 (1994).
- [23] J.P.Perdew, J.A.Chevary, S.H.Vorskov, K.A.Jackson, M.R.Pederson, D.J.Sinh, C.Fiolhais; *Phys.Rev.B*, **46**, 6671 (1992).
- [24] F.Viñes, F.Illas, K.M.Neyman; *J.Phys.Chem.A*, **112**, 8911 (2008).
- [25] P.Bloch; *Phys.Rev.B*, **50**, 17953 (1994).
- [26] G.Kresse, D.Joubert; *Phys.Rev.B*, **59**, 1758 (1999).
- [27] H.J.Monkhorst, J.D.Pack; *Phys.Rev.B*, **13**, 5188 (1976).
- [28] M.Methfessel, A.T.Paxton; *Phys.Rev.B*, **40**, 3616 (1986).
- [29] S.M.Kozlov, I.V.Yudanov, H.A.Aleksandrova, N.Rösch; *Phys.Chem.Chem.Phys.*, **11**, 10855 (2009).
- [30] I.V.Yudanov, A.V.Matveev, K.M.Neyman, Rösch; *N.J.Am.Chem.Soc.*, **130**, 9342 (2008).
- [31] J.-F.Paul, P.J.Sautet; *Phys.Chem.B*, **102**, 1578 (1998).
- [32] S.Stolbov, F.Mehmood, T.S.Rahman, M.Alatalo, I.Makkonen, P.Salo; *Phys.Rev.B*, **70**, 155410 (2004).
- [33] F.Mehmood, S.Stolbov, T.S.Rahman; *J.Phys. Condens.Matter*, **18**, 8015 (2006).
- [34] B.Hammer, J.K.Nørskov; *Surf.Sci.*, **343**, 211 (1995).